FFLO or Majorana superfluids: The fate of fermionic cold atoms in spin-orbit coupled optical lattices

Chunlei Qu^1 , Ming $Gong^1$, and Chuanwei $Zhang^{1*}$ ¹ Department of Physics, The University of Texas at Dallas, Richardson, TX, 75080 USA

The recent experimental realization of spin-orbit coupling (SOC) for ultra-cold atoms opens a completely new avenue for exploring new quantum matter. In experiments, the SOC is implemented simultaneously with a Zeeman field. Such spin-orbit coupled Fermi gases are predicted to support Majorana fermions with non-Abelian exchange statistics in one dimension (1D). However, as shown in recent theory and experiments for 1D spin-imbalanced Fermi gases, the Zeeman field can lead to the long-sought Fulde-Ferrell-Larkin-Ovchinnikov (FFLO) superfluids with non-zero momentum Cooper pairings, in contrast to the zero momentum pairing in Majorana superfluids. Therefore a natural question to ask is which phase, FFLO or Majorana superfluids, will survive in spin-orbit coupled Fermi gases in the presence of a large Zeeman field. In this paper, we address this question by studying the mean field quantum phases of 1D (quasi-1D) spin-orbit coupled fermionic cold atom optical lattices.

PACS numbers: 03.75.Ss, 67.85.-d, 74.20.Fg

I. INTRODUCTION

Spin-orbit (SO) coupling plays an important role in many important condensed matter phenomena [1, 2], ranging from spintronics to topological insulators. The recent experimental breakthrough in realizing SO coupling in ultra-cold Bose and Fermi gases [3–7] provides a new platform for engineering many new many-body quantum matters [8]. In the experiments, the SO coupling is realized together with a Zeeman field. It is well known that such SO coupling and Zeeman field, together with the s-wave superfluid pairing in degenerate Fermi gases, can support zero-energy Majorana fermions [9] with non-Abelian exchange statistics when the Zeeman field is beyond a certain critical value [10, 11]. In solid state, the same ingredient has been realized using a heterostructure composed of a semiconductor nanowire (or thin film) with strong SO coupling, an s-wave superconductor, and a magnetic field (or a magnetic insulator) [12–19]. Important experimental progresses have been made along this direction [20–23], where some signatures which may be related with Majorana fermions have been observed. In the solid state heterostructure, the s-wave pairing is induced to the semiconductor through proximity effects [24, 25].

In degenerate fermi gases, however, as observed in both theory and experiments [26–28], the presence of a large Zeeman field (realized by the spin population imbalance) can induce non-zero momentum Cooper pairings between atoms, i.e., FFLO phases [29–31], especially in low-dimensional Fermi gases. Such FFLO phases may not support Majorana fermions. Therefore it is natural to ask whether the FFLO superfluids [32–39] with non-zero momentum Cooper pairs or the Majorana superfluids with zero momentum Cooper pairs will survive

in the presence of SO coupling and a large Zeeman field. This question becomes especially important because of the recent experimental realization of SO coupled Fermi gases [6, 7], which makes the observation of Majorana fermions in cold atomic systems tantalizingly close. The cold atom system may be a better platform for the observation of Majorana fermions because of the lack of disorder and impurity [36, 40–45], an issue that has led to intensive debate in the condensed matter community on the zero-bias peak signature of Majorana fermions in recent transport experiments [20, 21].

In this paper, we address the competition between FFLO and Majorana superfluids by studying the quantum phases of spin-imbalanced Fermi gases in spin-orbit coupled optical lattices. Because of the fact that the experimentally realized SO coupling is one-dimensional (1D) and the natural dimension requirement for the realization of Majorana fermions in this system, we consider 1D SO coupled optical lattices (similar to 1D nanowires) and investigate the quantum phase diagram at zero temperature using the mean field theory. The quantum phases of Fermi atoms are obtained by self-consistently solving the corresponding Bogoliubov-de Gennes (BdG) equation. Without SO coupling, there are no Majorana superfluids, and FFLO superfluids appear in the large Zeeman field region. The SO coupling enhances the Majorana superfluid phase while suppresses the FFLO superfluid phase. Majorana and FFLO superfluids exist for different filling factors (i.e., in different chemical potential region). We characterize different quantum phases by visualizing their real space superfluid order parameters, density distributions, and Majorana zero energy wavefunctions. The effects of the harmonic trap are also discussed. We find that the same quantum phases are preserved in a 3D optical lattice with weak tunnelings along two transversal directions (quasi-1D geometry).

The rest of the paper is organized as follows. In Sec. II, we present the BdG equation for describing Fermi atoms in spin-orbit coupled optical lattices. The sym-

^{*} Corresponding author, Email:chuanwei.zhang@utdallas.edu

metry of the BdG equation and its consequence to the phase diagram is discussed. In Sec. III, we present the main numerical results obtained by self-consistently solving the BdG equation. We discuss the phase diagram, the characterization of various phases, and the effects of the harmonic trap and Hartree shift. We also present the results in a 3D optical lattice with weak tunnelings along two transversal directions. Sec. IV consists of discussion and conclusion.

II. HAMILTONIAN AND SYMMETRY

We consider a 1D degenerate Fermi gas with Zeeman field and SO coupling in an optical lattice. The dynamics of this system can be described by the standard tight-binding Hamiltonian

$$\mathcal{H} = \mathcal{H}_0 + \mathcal{H}_Z + \mathcal{H}_{SO},\tag{1}$$

where the first term is the usual spin-1/2 Fermi-Hubbard model in an optical lattice,

$$\mathcal{H}_{0} = -t \sum_{i\sigma} (\hat{c}_{i\sigma}^{\dagger} \hat{c}_{i+1\sigma} + H.c.) - \mu \sum_{i\sigma} \hat{n}_{i\sigma} - U \sum_{i} \hat{n}_{i\uparrow} \hat{n}_{i\downarrow},$$
(2)

t is the hopping amplitude, μ is the chemical potential, and U is the contact interaction. The second and third terms are the Zeeman field

$$\mathcal{H}_Z = -h \sum_{i} (\hat{c}_{i\uparrow}^{\dagger} \hat{c}_{i\uparrow} - \hat{c}_{i\downarrow}^{\dagger} \hat{c}_{i\downarrow})$$

and SO coupling

$$\mathcal{H}_{SO} = \alpha \sum_{i} (\hat{c}_{i-1,\uparrow}^{\dagger} \hat{c}_{i\downarrow} - \hat{c}_{i+1,\uparrow}^{\dagger} \hat{c}_{i\downarrow} + H.c.).$$

Such type of SO coupling and Zeeman field have been realized in recent experiments for both bosons and fermions [3–7]. In experiments, the hopping amplitude, Zeeman field, SO coupling strength, and contact interactions may be tuned independently. In our numerical simulation we set t=1 throughout this work. All other energies are scaled by t. The total length of the 1D optical lattice is chosen as N=100, which is long enough to ensure that the coupling between two ends is vanishingly small. An open boundary condition is used to obtain the zero-energy Majorana fermions at two ends of the 1D optical lattice in the topological superfluid regime.

As the first approach for understanding the quantum phases of such 1D SO coupled optical lattices, we consider the standard mean field theory. We decouple the interaction term in H_0 using

$$-U\hat{n}_{i\uparrow}\hat{n}_{i\downarrow} = \Delta_{i}\hat{c}_{i\uparrow}^{\dagger}\hat{c}_{i\downarrow}^{\dagger} + \Delta_{i}^{*}\hat{c}_{i\downarrow}\hat{c}_{i\uparrow} - |\Delta_{i}|^{2}/U +U\langle\hat{n}_{i\uparrow}\rangle\hat{n}_{i\downarrow} + U\hat{n}_{i\uparrow}\langle\hat{n}_{i\downarrow}\rangle - U\langle\hat{n}_{i\uparrow}\rangle\langle\hat{n}_{i\downarrow}\rangle.$$

Notice that here we have taken into account the Hartree shift term, which has quantitative effects on our results.

The effective Hamiltonian reads as

$$\mathcal{H}^{\text{eff}} = -t \sum_{i} \sum_{\sigma} (\hat{c}_{i\sigma}^{\dagger} \hat{c}_{i+1\sigma} + H.c.) - \sum_{i\sigma} \tilde{\mu}_{i\sigma} \hat{c}_{i\sigma}^{\dagger} \hat{c}_{i\sigma}$$

$$+ \sum_{i} (\Delta_{i} \hat{c}_{i\uparrow}^{\dagger} \hat{c}_{i\downarrow}^{\dagger} + \Delta_{i}^{*} \hat{c}_{i\downarrow} \hat{c}_{i\uparrow}) + \mathcal{H}_{Z} + \mathcal{H}_{SO},$$
 (3)

where the chemical potential $\tilde{\mu}_{i\sigma} = \mu + U\langle \hat{n}_{i\bar{\sigma}} \rangle$ becomes site dependent, $\bar{\sigma} = -\sigma$. The superfluid pair potential is defined as $\Delta_i = -U\langle \hat{c}_{i\downarrow}\hat{c}_{i\uparrow} \rangle$. Using the Bogoliubov transformation $\hat{c}_{i\sigma} = \sum_n (u_{i\sigma}^n \hat{\Gamma}_n - \sigma v_{i\sigma}^n \hat{\Gamma}_n^{\dagger})$, we obtain the BdG equation

$$\sum_{j} \begin{pmatrix} H_{ij\uparrow} & \alpha_{ij} & 0 & \Delta_{ij} \\ -\alpha_{ij} & H_{ij\downarrow} & -\Delta_{ij} & 0 \\ 0 & -\Delta_{ij}^* & -H_{ij\uparrow} & -\alpha_{ij} \\ \Delta_{ij}^* & 0 & \alpha_{ij} & -H_{ij\downarrow} \end{pmatrix} \begin{pmatrix} u_{j\uparrow}^n \\ u_{j\downarrow}^n \\ -v_{j\uparrow}^n \\ v_{j\downarrow}^n \end{pmatrix} = E_n \begin{pmatrix} u_{j\uparrow}^n \\ u_{j\downarrow}^n \\ -v_{j\uparrow}^n \\ v_{j\downarrow}^n \\ v_{j\downarrow}^n \end{pmatrix},$$

where $H_{ij\uparrow} = -t\delta_{i\pm 1,j} - (\tilde{\mu}_{i\sigma} + h)\delta_{ij}, H_{ij\downarrow} = -t\delta_{i\pm 1,j} - (\tilde{\mu}_{i\sigma} - h)\delta_{ij}, \alpha_{ij} = (j-i)\alpha\delta_{i\pm 1,j},$

$$\Delta_{ij} = -U\delta_{ij} \sum_{n=1}^{2N} [u_{i\uparrow}^n v_{i\downarrow}^{n*} f(E_n) - u_{i\downarrow}^n v_{i\uparrow}^{n*} f(-E_n)], \quad (5)$$

$$\langle \hat{n}_{i\uparrow} \rangle = \sum_{n=1}^{2N} [|u_{i\uparrow}|^2 f(E_n) + |v_{i\uparrow}|^2 f(-E_n)],$$

$$\langle \hat{n}_{i\uparrow} \rangle = \sum_{n=1}^{2N} [|u_{i\downarrow}|^2 f(E_n) + |v_{i\downarrow}|^2 f(-E_n)], \qquad (6)$$

with the Fermi-Dirac distribution $f(E)=1/\left(1+e^{E/T}\right)$. The BdG equation (4) should be solved self-consistently with the order parameter equation (5) and the particle number equation (6) for the average number of atoms per lattice site $n=\sum_{i,\sigma}\left\langle\hat{n}_{i\sigma}\right\rangle/N$. Here we denote n as the filling factor for convenience (note that generally the filling factor is defined as $\nu=n/2$ in the literature). In our simulation, we take the attractive interaction strength U=4.5 and the temperature T=0.

The original Hamiltonian Eq. (1) contains no imaginary part, therefore the wavefunction in Eq. (4) can be made real and the order parameter in Eq. (3) is also real. The topological symmetry of the effective model belongs to BDI class, with characteristic index \mathcal{Z} , instead of the BdG D-class with \mathcal{Z}_2 index [40, 46]. The mean field Hamiltonian (3) still preserves the basic symmetry properties of Eq. (1). Consider the particle-

hole operation
$$C\begin{pmatrix} \hat{c}_{i\uparrow} \\ \hat{c}_{i\downarrow} \end{pmatrix}C^{-1} = (-1)^i \begin{pmatrix} \hat{c}_{i\uparrow}^{\dagger} \\ \hat{c}_{i\downarrow}^{\dagger} \end{pmatrix}$$
, we have

 $\mathcal{C}H(\mu)\mathcal{C}^{-1}=H(-\mu)$ when the Hartree shift term is ignored and $\mathcal{C}H(\mu)\mathcal{C}^{-1}=H(-U-\mu)$ when the Hartree shift term is included. Thus the spectrum should be symmetric about $\mu=0$ and $\mu=-\frac{U}{2}$ respectively, which is confirmed in our numerical results (see Fig. 1 and Fig. 6). However, in the presence of a trapping potential, the chemical potential becomes site dependent, thus the particle-hole symmetry $\mathcal C$ is broken and the band structure is no longer symmetric about $\mu=0$ (see Fig. 5).

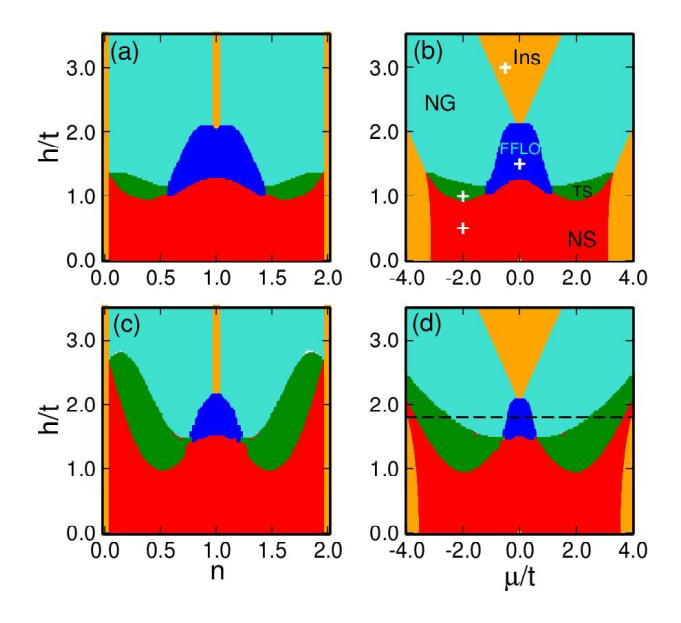


FIG. 1. (Color online) Phase diagram of 1D SO coupled optical lattices as a function of Zeeman field h and filling factor n (a,c) or chemical potential μ (b,d). First row: the spin orbit coupling $\alpha=0.5$, second row: $\alpha=1.0$. Five different phases are identified in each phase diagram: normal BCS superfluid (NS), topological superfluid (TS), FFLO, normal gas (NG), and insulator phase (Ins).

III. PHASE DIAGRAM: MAJORANA VERSUS FFLO SUPERFLUIDS

We self-consistently solve the BdG equations (4,5,6) with an open boundary condition to obtain the phase diagram. The SO coupled optical lattice supports several different phases: normal BCS superfluid (NS) with $\Delta \neq 0$ and all non-zero eigenstates; topological superfluids with $\Delta \neq 0$ and zero-energy Majorana fermions located at two ends of the lattice; FFLO phase with oscillating Δ and magnetization; insulator phase (Ins) with integer filling factor and finite energy gaps; and normal gas (NG) phase without pairing and energy gap. We first study the phases without Hartree shift, and address the role of Hartree shift at the end of the section.

A. Phase diagram without Hartree shift

Our numerical results are presented in Fig. 1 for two different sets of SO coupling strength. In Figs. 1 (a) and (c) we plot the phase diagram in the h-n plane and in Figs. 1 (b) and (d) we plot the results in the $h-\mu$ plane. We see the phase diagram is symmetric around n=1 or $\mu=0$, as discussed in the previous section. When the Zeeman field h is very small, the system favors the normal BCS superfluids. With increasing Zeeman field h, topological superfluids and FFLO phases emerge as the ground states of the system for different filling factors. The FFLO phase is more likely to be observed around

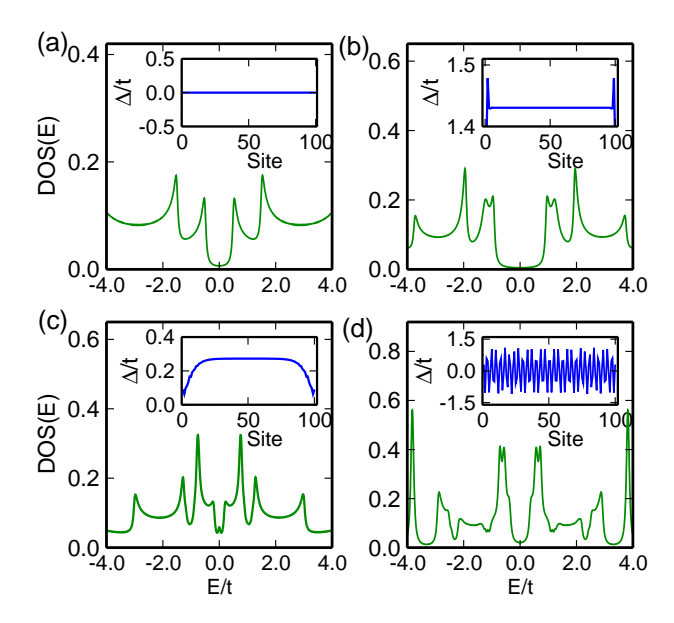


FIG. 2. (Color online) Representative density of states for (a) insulator phase, (b) normal BCS superfluid phase, (c) topological superfluid phase, and (d) FFLO phase. The insets show the order parameters in each phase. The corresponding phase points are marked by the plus signs in Fig. 1b. Note that there is a zero-energy peak in the DOS in the topological superfluid phase as shown in (c).

the integer filling factor n=1. When the Zeeman field becomes even larger, where only atoms with one type of spin can stay in each lattice site, the insulator phase develops with the filling factor n=1. The insulator phase can also be found when μ is too large (fully occupied band) or to small (empty band). The topological phase and associated Majorana fermions emerge with fractional filling factors n. By comparing the phase region for different SO coupling, we find that the SO coupling enhances the topological superfluid phase and suppresses the FFLO phase. Note that without SO coupling, there is only FFLO phase, and no topological superfluid phase [26, 27].

Different quantum phases in Fig. 1 can be characterized by different density of states (DOS) $\rho(E) =$ $\sum [|u_{i\sigma}|^2 \delta(E-E_n) + |v_{i\sigma}|^2 \delta(E+E_n)]$ and superfluid order parameter $\Delta(x)$, as shown in Fig. 2. In the insulator phase (Fig. 2a), the order parameter $\Delta = 0$ and there is an energy gap for excitations. In the normal BCS superfluid phase (Fig. 2b), the order parameter is non-zero and there is a superfluid gap around E=0. In the topological superfluid phase (Fig. 2c), a zero energy peak appears in the DOS which corresponds to the zero energy Majorana state. Note that for the normal BCS superfluid phase the order parameter has a strong oscillation near each end, while for the topological superfluid, the order parameters is a monotonic function of the sites. Similar features have always been found for these two different phases for different parameters. The FFLO phase (Fig. 2d) is characterized by the spatially oscillating order parameter and

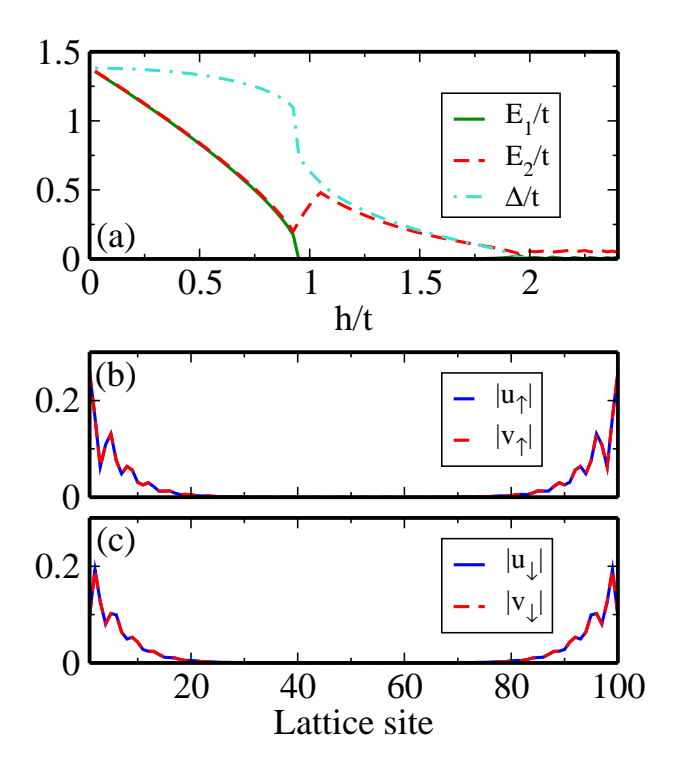


FIG. 3. (Color online) (a) Plot of the order parameter and the lowest two eigenenergies E_1 and E_2 as a function of Zeeman field for the transition from normal BCS superfluids to topological superfluids. $\alpha = 1.0, \mu = -2.0$. (b,c) The Majorana zero energy state wavefunction.

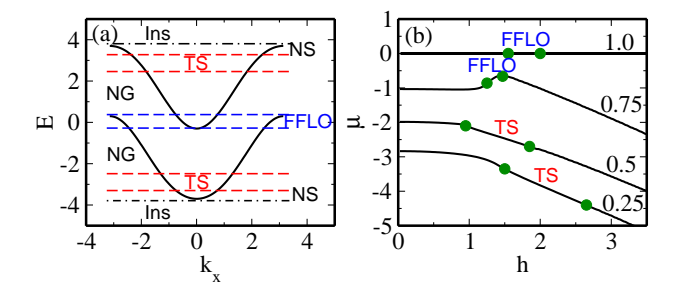


FIG. 4. (Color online) Single particle band structure of the spin-orbit coupled optical lattices. $\alpha=1.0,\ h=1.7$ (corresponds to the dashed line in Fig. 1d). Corresponding chemical potential regions for different phases are identified. (b) Plot of μ as a function of Zeeman field for fixed filling factor $n=0.25,\ 0.5,\ 0.75,\ 1.0$. The regions between the two circle symbols on each line label the topological superfluid phase (for $n=0.25,\ 0.5$) or the FFLO phase (for $n=0.75,\ 1.0$).

the excitations are always gapless.

The emergence of Majorana zero energy state at the ends of the SO coupled optical lattices can be clearly seen in Fig. 3. In Fig. 3 we plot the bulk order parameter, the first and second non-negative eigenvalues, denoted by E_1 and E_2 , of the BdG equation as a function of Zeeman field. We see that in the normal BCS superfluid regime E_1 is always equal to E_2 , and smaller than the order parameter. The energy gap not equal to the order parameter

eter is a unique feature for spin-orbit coupled systems. When h approach 1.0 ($h > \Delta$), we observe a sudden jump of the order parameter and the system enters the topological superfluid regime, where $E_1 = 0$, and E_2 increases and reaches the maximum value 0.5 at $h \sim 1.1t$. When h further increases, $E_2 \sim \Delta$ gradually decreases and becomes zero when the system enters the normal gas phase. In the topological superfluid phase, E_2 is the minimum energy gap that protects the topological zero energy Majorana state. In Fig. 3b and c, we plot zero energy state, which is the eigenstate of the Bogoliubov quasiparticle operators $\Gamma_0^{\dagger} = \sum_{i\sigma} (u_{i\sigma}^0 c_{i\sigma}^{\dagger} + v_{i\sigma}^0 c_{i\sigma})$. The eigenstates satisfy that $u_{i\sigma} = v_{i\sigma}$ on one end and $u_{i\sigma} = -v_{i\sigma}$ on the other end. Thus by defining $\Gamma_0^{\dagger} = \gamma_L + i\gamma_R$, we could identify the left and right end Majorana Fermions $\gamma_{L(R)}$.

Different phases in different parameter regions can be intuitively understood from the single particle band structure, as shown in Fig. 4a for $\alpha=1,\ h=1.7$ (corresponds to the dashed line in Fig. 1d). The chemical potential regions for different phases are identified in the figure. Comparing Fig. 1d and Fig. 4a, we see the topological superfluid phase appears when the chemical potential cuts only a single band, while the FFLO phase appears mainly around $\mu=0$ (filling factor n=1) and cuts two bands. The insulator phase appears when two bands are either both fully occupied or empty. Normal superfluid or normal gas phases also appear when a single band is occupied with either small or large filling factors.

Because of the SO coupling, the spin polarization is not a conserved quantity anymore, which is different from the spin-imbalanced Fermi gases in the literature. However, the filling factor can still be controlled precisely in experiments. With increasing Zeeman field, the chemical potential changes for a fixed filling factor, leading to the transition between different phases. In Fig. 4b we plot the chemical potential as a function of Zeeman field for different filling factor n. Generally when n < 0.7or n > 1.3, we find μ changes monotonically as a function of the Zeeman field. However, in the case n = 0.75, the chemical potential does not change when h < 1 and then increases slightly when the system enters the FFLO phase regime. For n = 1, the chemical potential is independent of the filling factor due to the particle-hole symmetry. Notice that n is not a unique function of the chemical potential, therefore in Fig. 1 we see that the FFLO phase is very large in the h-n plane but becomes much smaller in the $h - \mu$ plane because the mapping is a very complex function.

B. Phase diagram in a harmonic trap

In a realistic experiment, a harmonic trapping potential $V(x) = \frac{1}{2}\omega_x^2(i-L_c)^2$ exists, where ω_x is the trapping frequency and L_c is the center of the lattice. The effects of the trapping potential on the filling factor and order parameter are shown in Fig. 5(a) and (b). With increasing trapping frequency, the ultracold atoms are forced to

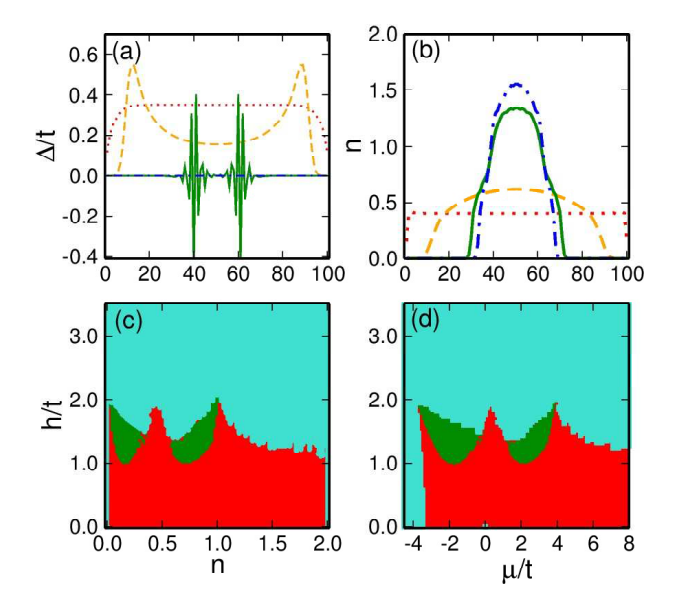


FIG. 5. Phase diagram in the presence of a harmonic trap. The order parameter profiles (a) and atom density distributions (b) for different trapping frequencies: $\omega_x = 0.0$ (Red dotted line), 0.05 (Orange dashed line), 0.15 (Green solid line), and 0.2 (Blue dash-dotted line). (c) and (d) are phase diagram as a function of Zeeman field h and filling factor n or chemical potential μ .

the center of the trap which has a lower potential. With a high trapping frequency, a shell structure is developed, where superfluid, insulator, and normal gas phases appear in different regions of the harmonic trap. In the superfluid regime in the trap, topological superfluid or FFLO phase may develop for different parameters. In Fig. 5 (c) and (d) we plot the phase diagram for a fixed trapping potential. Notice that there is always a mixture of different phases in the trap, therefore we only identify three different cases in our plot: normal gas for the whole lattice, topological superfluids (with zero-energy Majorana fermions) and other superfluids (normal BCS superfluids or FFLO) in certain part of the lattice. In the topological superfluid, the Majorana wavefunction does not localize at the two ends of the trap, but in certain middle region of the trapping potential [37]. The position of the Majorana fermion changes with the trapping frequency. With the trapping potential, the effective chemical potential is site-dependent, therefore the particle-hole symmetry is broken and the phase diagram is not symmetric with respect to n=1 (Fig. 5 (c)) or $\mu=0$ (Fig. 5 (d)).

C. Effect of Hartree shift

We also study the effect of the Hartree shift on the phase diagram. When the Hartree shift is included, the local chemical potential and Zeeman field are both modified as seen from $\tilde{\mu}_{i\sigma} = \mu + U \langle n_{i\bar{\sigma}} \rangle$. If we define $\langle n_i \rangle$

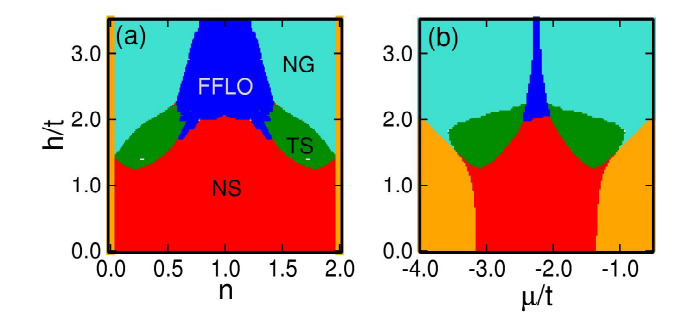


FIG. 6. Phase diagram with the inclusion of the Hartree shift. $\alpha=0.5$. All other parameters and notations are the same as that in Fig. 1.

and $\langle m_i \rangle$ as the local particle number and magnetization $m_i = n_{i\uparrow} - n_{i\downarrow}$, then the modified chemical potential and Zeeman field with including the Hartree shift term will be $\mu_i = \mu + U\langle n_i \rangle$ and $h_i = h - \frac{U}{2}\langle m_i \rangle$. The numerical results are presented in Fig. 6 for a direct comparison with the results without Hartree shift (Fig. 1 (c) and (d)). We see the phase diagram is still qualitatively the same except that now the phase diagram is symmetric for $\mu = -U/2$ as discussed in the above. Since the Zeeman field h_i depends strongly on the local magnetization m_i and the FFLO phase is a competition between superfluid and magnetization, it is hard to numerically determine FFLO phases near the phase boundary between FFLO and topological superfluid phases. This is because the total free energy becomes extremely complex as a function of order parameters and other quantities, and most solutions we find correspond to excited states, instead of global minimum of the free energy. Thus the boundary between topological superfluid and FFLO phase cannot be determined precisely.

D. Quantum phases in quasi-1D lattices

In a truly 1D system, quantum fluctuations become significant and need be taken into account, which are beyond our mean field approximation. The effects of quantum fluctuations can be suppressed by considering a three-dimensional lattice with weak coupling $t_{\perp} = 0.1t$ along two transversal directions, similar as the high temperature cuprate superconductor where 2D superconductivity is stabilized by weak coupling along the third direction. In experiments, such setup can be realized in 3D degenerate Fermi gases subject to 2D strong optical lattices, forming weakly coupled 1D tube arrays. The 1D weak lattice and spin-orbit coupling are then applied on each tube. The quantum phases in the quasi-1D system are calculated by self-consistently solving the corresponding BdG equations and are found to be similar to the above 1D results. Here we focus on the interesting topological and FFLO phases. The order parameters

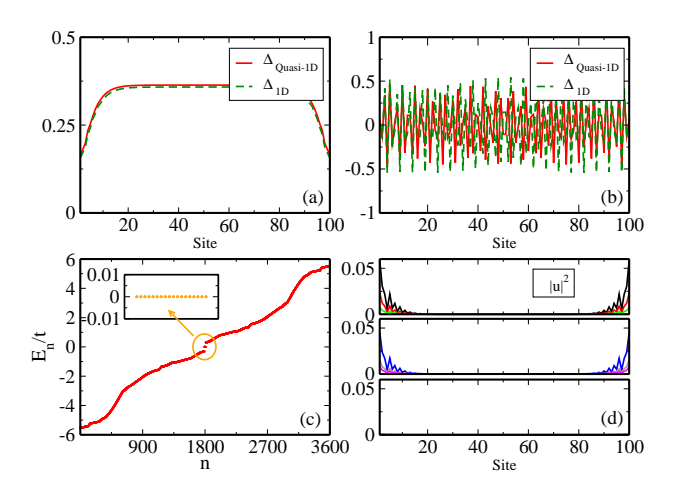


FIG. 7. Topological and FFLO phases in a quasi-1D (100 \times 3 \times 3) lattice. (a,b) The order parameters in topological superfluid (a) and FFLO (b) phases. Red solid lines: quasi-1D; Green dashed lines: 1D for the same parameters. (c) The BdG excitation spectrum in the topological superfluid phase. The inset shows the nine zero energy states (18 shown due to the finite size effect that lift the degeneracy slightly). (d) The corresponding edge state wavefunction along nine tubes of the quasi-1D lattice for one of the zero energy states. Parameters: $V_z = 1.2$, $\mu = -2$ for the topological superfluid phase and $V_z = 1.8$, $\mu = 0$ for the FFLO phase.

of these two phases in quasi-1D lattices are shown in Figs. 7 (a) and (b). Comparing to 1D results, the order parameters only change slightly due to the week tunneling between tubes. In contrast to 1D lattices, the array of lattice tubes can host multiple Majorana zero energy states at the ends of each tube, as shown in Fig. 7 (c) for the Bogoliubov excitation spectrum. However, the weak

tunnelings do not lift the zero energy degeneracy because they are along the traversal directions, which are different from the strong energy splitting induced by the coupling between two Majorana fermions in the same tube due to the short tube length. The zero energy wavefunctions are still localized around the edges of the tubes, but can expand along the transversal directions due to the weak tunneling, as shown in Fig. 7d.

IV. CONCLUSION

In summary, in this paper, we address the question that which phases, FFLO or Majorana superfluids, will survive in spin-orbit coupled Fermi gases in the presence of a large Zeeman field through studying the mean field quantum phases of 1D and quasi-1D spin-orbit coupled optical lattices. In the optical lattice system each site can host at most 2 fermions, making the system host plenty of phases depending on the filling factor and the Zeeman field, which are quite different from the free space results. At a finite Zeeman field we observe the strong competition between topological superfluid phase and FFLO phase. The SO coupling enhances the topological superfluid phase while suppresses the FFLO phase. The weak tunneling along transversal directions in quasi-1D lattices does not change the results. These results are not only important for the search of Majorana fermions in spinorbit coupled degenerate Fermi gases, but may also have significant applications for the solid state nanowire heterostructures where similar physics exists.

Acknowledgement: The authors acknowledge the supported by ARO (W911NF-12-1-0334), AFOSR (FA9550-13-1-0045), and NSF-PHY (1104546).

- M. Z. Hasan and C. L. Kane, Rev. Mod. Phys. 82, 3045 (2010).
- [2] X.-L. Qi and S.-C. Zhang, Rev. Mod. Phys. 83, 1057 (2011).
- [3] Y.-J. Lin, K. Jiménez-García, and I. B. Spielman, Nature **471**, 83 (2011).
- [4] J. Y. Zhang, S. C. Ji, Z. Chen, et. al, Phys, Rev. Lett. 109, 115301 (2012).
- [5] C. Qu, C. Hamner, M. Gong, et. al, arXiv:1301.0658 (2013).
- [6] P. Wang, Z.-Q. Yu, Z. Fu, et. al, Phys. Rev. Lett. 109,095301 (2012).
- [7] L. W. Cheuk, A. T. Sommer, Z. Hadzibabic, et. al, Phys. Rev. Lett. 89, 095302(2012).
- [8] V. Galitski, and I. B. Spielman, Nature **494**, 49 (2013).
- [9] C. Zhang, S. Tewari, R.M. Lutchyn, and S. Das Sarma, Phys. Rev. Lett. 101, 160401 (2008).
- [10] A. Kitaev, Ann. Phys. (N.Y.) **303**, 2 (2003).
- [11] C. Nayak, S.H. Simon, A. Stern, et. al, Rev. Mod. Phys. 80, 1083 (2008).
- [12] L. Fu and C. L. Kane, Phys. Rev. Lett. 100, 096407 (2008).

- [13] J. D. Sau, R. M. Lutchyn, S. Tewari, et. al, Phys. Rev. Lett. 104, 040502 (2010).
- [14] J. D. Sau, S. Tewari, R. M. Lutchyn, et. al, Phys. Rev. B 82, 214509 (2010).
- [15] J. Alicea, Phys. Rev. B 81, 125318 (2010).
- [16] R. M. Lutchyn, J. D. Sau, and S. Das Sarma, Phys. Rev. Lett. 105, 077001 (2010).
- [17] Y. Oreg, G. Refael, and F. von Oppen, Phys. Rev. Lett. 105, 177002 (2010).
- [18] A. C. Potter and Patrick A. Lee, Phys. Rev. Lett. 105, 227003 (2010).
- [19] L. Mao, M. Gong, E. Dumitrescu, et. al, Phys. Rev. Lett. 108, 177001 (2012).
- [20] V. Mourik, K. Zuo, S. M. Frolov, et. al, Science, 336, 1003 (2012).
- [21] A. Das, Y. Ronen, Y. Most, et. al, Nature Physics 8, 887 (2012).
- [22] M. T. Deng, C. L. Yu, G. Y. Huang, et. al, Nano Lett. 12, 6414 (2012).
- [23] L. P. Rokhinson, X. Liu, and J. K. Furdyna, Nature Physics 8, 795 (2012).
- [24] Y. J. Doh, J. A. Dam, A. L. Roest, et. al, Science 309,

- 272 (2005).
- [25] J. Xiang, A. Vidan, M. Tinkham, et. al, Nature Nanotechnology 1, 208 (2006).
- [26] M. R. Bakhtiari, M.J. Leskinen, and P. Torma, Phys. Rev. Lett. 101, 120404 (2008).
- [27] Y. L. Loh and N. Trivedi, arXiv:0907.0679
- [28] Y.-A. Liao, A. S. Rittner, T.Paprott, et. al, Nature, 467, 567 (2010).
- [29] P. Fulde, and R.A. Ferrell, Phys. Rev. 135, A550 (1964).
- [30] A.I. Larkin, and Yu.N. Ovchinnikov, Zh. Eksp. Teor. Fiz. 47, 1136 (1964).
- [31] A.I. Larkin, and Yu,N. Ovchinnikov, Sov. Phys. JETP 20, 762 (1965).
- [32] M. Iskin, Phys. Rev. A 86, 065601 (2012).
- [33] Z. Zheng, M. Gong, X. Zou, C. Zhang, and G.-C. Guo, Phys. Rev. A 87, 031602(R) (2013).
- [34] X.-J. Liu and H. Hu, arXiv:1302.0553 (2013).
- [35] L. Dong, L. Jiang, and H. Pu, arXiv:1302.1189 (2013).
- [36] X.-J. Liu, L. Jiang, H. Pu, and H. Hu, Phys. Rev. A 85,

- 021603(R)(2012);
- [37] X.-J. Liu and H. Hu, Phys. Rev. A 85, 033622(R)(2012);
- [38] F. Wu, G.-C. Guo, W. Zhang and Wei Yi, Phys. Rev. Lett. 110, 110401(2013).
- [39] Y. Xu, C. Qu, M. Gong, and C. Zhang, arXiv:1305.2152.
- [40] X. J. Liu, Z. X. Liu, and M. Cheng, Phys. Rev. Lett. 110, 076401 (2013).
- [41] L. Jiang, T. Kitagawa, J. Alicea, et. al, Phys. Rev. Lett. 106, 220402 (2011).
- [42] M. Gong, S. Tewari, and C. Zhang, Phys. Rev. Lett. 107, 195303 (2011).
- [43] M. Gong, G. Chen, S. Jia, C. Zhang, Phys. Rev. Lett. 109, 105302 (2012).
- [44] M. Sato, Y. Takahashi, and S. Fujimoto, Phys. Rev. Lett. 103, 020401 (2009).
- [45] S. L. Zhu, L. B. Shao, Z. D. Wang, et. al, Phys. Rev. Lett. 106, 100404 (2011).
- [46] S. Tewari, and J. D. Sau, Phys. Rev. Lett. 109, 150408 (2012).